Graphene Nano-Ribbon (GNR) Interconnects: A Genuine Contender or a Delusive Dream?

Chuan Xu, Hong Li and Kaustav Banerjee
Department of Electrical and Computer Engineering, University of California, Santa Barbara, CA 93106, USA
e-mail: {chuanxu, hongli, kaustav}@ece.ucsb.edu

Abstract

This paper presents a comprehensive conductance and delay analysis of graphene nano-ribbon (GNR) interconnects. The conductance model of GNR is derived using a simple tight binding model and the linear response Landauer formula. Several GNR structures are examined, and the conductance among them and other interconnect materials (copper, tungsten and carbon nanotubes) is compared. Impact of different model parameters (mean free path, Fermi level and edge specularity) on the conductance is discussed. An *RLC* equivalent circuit model is defined to analyze both global and local GNR interconnect delays. The results reveal that till the very end of ITRS'07 roadmap, GNRs cannot match the performance of global level copper or SWCNTs, unless multiple layers along with proper intercalation doping is used and specular nano-ribbon edge is achieved. However, multi-layer zigzag edged GNRs (zz-GNRs) can be comparable to copper at the local level, and can have much better performance than that of tungsten, implying possible application as local interconnects.

I. Introduction

Graphene nanoribbons (GNRs) have been recently proposed as one of the potential candidates for both transistors [1] and interconnects [2,3]. GNRs can be either semiconducting or metallic, depending on the geometry, similar to the carbon nanotubes (CNTs). Compared to Cu, a traditional interconnect material, both GNRs and CNTs have large carrier mean free path (MFP), and they can also conduct much larger current densities. Compared to CNTs, GNRs are believed to be more controllable from a fabrication point of view. This is due to the planar nature of graphene, which can be patterned using high-resolution lithography.

However, several issues also exist in GNRs. Firstly, GNRs have edge scattering, which reduces the effective MFP, while CNTs have no such issue. Secondly, while mono-layer graphene has large MFP and conductivity, multi-layer graphene turns to graphite and has much lower conductivity per layer due to inter-sheet electron hopping [4]. While various fabrication methods of GNRs are being pursued [5], there is a need to evaluate the applicability of GNR as VLSI interconnects and evaluate their performance in comparison to traditional metals (Cu and W) and CNTs. This will also provide guidance to the GNR interconnect fabrication processes. The conductance of GNRs has been modeled in previous works [2, 3]. Both metallic and semiconducting GNRs were modeled, and compared with Cu and single-walled CNTs (SWCNTs). However, there are serious deficiencies in these works. The assumption that armchair GNRs can be differentiated as metallic and semiconducting, implies that the number (N) of hexagonal carbon rings across the width of GNR is fixed everywhere along the length (either N=3p-1 (metallic) or N=3p, 3p+1 (semiconducting), where p is an integer [2, 3]), which further implies very smooth (specular) edges of GNRs, and is against the complete diffusive-edge assumption made in [2]. Although the above assumption is not against the complete specular-edge assumption in [3], theoretically, nano patterning down to the accuracy of 1 atom is a formidable task from a practical point of view [6]. Moreover, due to the high resistance of single graphene layers, it becomes necessary to use multiple graphene layers. Additionally, the conductance of GNRs can be modulated by doping. However, no detailed research effort has adequately addressed the conductance and/or delay modeling of multi-layer GNRs incorporating the effect of doping and edge specularity.

In this work, intercalation doping effects and edge specularity effect for multi-layer GNRs have been analyzed for the first time. The width dependence of the MFP in mono-layer GNRs is also taken into account. A realistic comparison among GNRs, CNTs, Cu (copper) and W (tungsten) is presented based on the interconnect geometry predicted in ITRS 2007 [7] for local and global level interconnects. An *RLC* delay model for GNR interconnects is also presented and used for comparative performance analysis.

II. Fundamental Physics and Models of GNR Conductance

Graphene is a flat mono-layer of carbon atoms tightly packed into a two dimensional (2D) honeycomb lattice, and is a basic building block of graphite, carbon nanotubes (CNTs), graphene nanoribbons (GNRs), etc [5]. GNRs are confined 1D structures. The band structures of armchair and zigzag edged GNRs (ac-GNRs and zz-GNRs) are calculated using a tight binding model [6] (**Fig. 1**). The conductance of GNRs is derived using the linear response Landauer formula [8] (**Eq 1**, **Fig. 2**). zz-GNRs are always metallic (according to **Fig. 1**), and the total conductance of a single GNR layer can be calculated as shown in (**Eq 3**, **Fig. 2**). ac-GNRs can be either metallic or semiconducting, depending on the number of hexagonal carbon rings across the width (W), as stated above. However, patterning ac-GNRs with the width accuracy of one atom is not practical. Therefore, the integration form (**Eq 4**, **Fig. 2**) of the total conductance is used for ac-GNRs (valid when $\Delta E_n = h v_f / 2W$ is smaller than $\max\{kT, |E_F|\}$). The resistance difference between zz-GNRs and ac-GNRs becomes negligible when GNR width is large enough (**Fig. 4a**). When $kT \ll |E_F|$, the derived expression for the 2D sheet conductance (**Eq 5**, **Fig. 2**) is also consistent with [4].

The mean free path (MFP), l_D, plays an important role in determining the conductance. In previous works [2, 3], an arbitrary fixed l_D of 1 μm corresponding to scatterings by defects and phonons is assumed, which is based on the experimental results of [9]. However, l_D = 1 μm is not a physical limit and can be improved as fabrication technology progresses. Moreover, the fixed l_D model for mono-layer GNRs is not consistent with the width-dependent l_D model for CNTs, due to the similar nature of GNRs and CNTs. In this paper, the width dependence of MFP is taken into account. This model is based on the theory that the MFP of mono-layer GNR is approximately proportional to their width [6], just like the MFP of CNTs is a function of their diameter [10, 11] (**Fig. 3**). As shown in **Fig. 4b**, the calculated resistance of GNRs using the width dependent MFP model of Fig. 3 predicts smaller resistances than those estimated using a fixed l_D of 1 μm (**Fig. 4a**). In the following analysis, the width dependent MFP model is assumed for the mono-layer GNRs, while fixed values of l_D are extracted for the multi-layer GNRs due to the fact that when graphene layers are stacked together, the MFP and conductance per layer is reduced because of intersheet electron hopping [4], which is independent of width. Also, it can be observed from **Fig. 4** that the resistance of zz-GNRs is smaller than that of the corresponding ac-GNRs if W < 45 nm. Since this paper focuses on the possible application of GNRs as future VLSI interconnects, the following analysis will only discuss zz-GNRs.

III. RLC Delay Model for GNR Interconnects

Besides the resistance, the capacitance and inductance are also important to the propagation delay. Similar to the CNTs, the distributed capacitance of GNRs contains both the electrostatic and quantum capacitances, while the distributed inductance contains both the magnetic and kinetic inductances. The distributed *RLC* model for GNRs

is defined in **Fig. 5**. Generally, the kinetic inductance in mono-layer GNRs is much larger than the magnetic inductance, while the quantum capacitance in multi-layer GNRs is much larger than the electrostatic capacitance.

IV. Performance Comparison of GNRs with other Materials

Different structures of GNRs (**Fig. 6**) for possible interconnect applications are simulated. The MFP of neutral graphite is extracted as 419 nm from the in-plane conductivity of 0.026 $(\mu\Omega cm)^{-1}$ and layer spacing of 0.34 nm (set $E_F = 0$ in **Eq 5**, **Fig. 2**). The in-plane conductivity of graphite can be increased by several tens of magnitude by intercalation doping, because doping can increase the carrier density due to charge transfer and increase the MFP due to increased layer spacing (interlayer scattering is suppressed) [12]. For example, the stage 2 AsF_5 intercalated graphite can have in-plane conductivity of 0.63 $(\mu\Omega cm)^{-1}$, which is slightly greater than the bulk conductivity of Cu, with a hole density of 4.6×10^{20} cm^{-3} and average layer spacing of 0.575 nm [13,14]. This results in $|E_F| = 0.60$ eV and $l_D = 1.03$ μm. In addition to the GNRs, copper (Cu), SWCNT bundles, and tungsten (W) are also discussed in this section for comparison. The geometry of the wires and the resistivity for Cu wire is obtained from the ITRS roadmap [7]. The resistance model for SWCNT bundles is shown in **Fig. 7** [11], while the resistivity model for tungsten wire is shown in **Fig. 8** [15,16].

Beyond the 22 nm tech. node, according to the resistance comparison (**Fig. 9**), SWCNT bundles are the best, while all of the GNR structures are not better than Cu—for both global and local wires. However, AsF_5 doped multi-layer GNR is always better than tungsten. It should be noted that larger conductivity (~1 $(\mu\Omega cm)^{-1}$) of intercalated graphite has been reported in [17], however, further analysis is required to determine whether it is suitable for GNR, because large conductivity for bulk graphite does not necessarily mean a large conductance for multi-layer zz-GNR: the conductance for multi-layer zz-GNRs is dependent on many parameters such as layer spacing, l_D, E_F, edge specularity (p), the wire width and the wire length.

Fig. 10 shows the conductance contour plots as a function of both l_D and E_F for both bulk graphite and 16.5 nm wide (minimum global wire width for 11 nm tech. node) multilayer zz-GNRs. The plots indicate that l_D is more important than E_F for very narrow zz-GNRs (conductance does not change significantly with E_F), but they are equally important for bulk graphite.

Another way to improve the GNR conductance is to improve the specularity (p) of the edges. This can be modeled by multiplying the term $1/W\cot\theta$ in **Eq 2**, **Fig. 2** by $(1-p)$. While the conductance of multi-layer zz-GNRs, with intercalation doping, can be improved significantly if the edges change from completely diffusive (p=0) to completely specular (p=1), conductance of neutral multi-layer zz-GNRs does not improve (**Fig. 11(a)**). This is due to the following four reasons: (i) the conductance of the zeroth conduction modes ($E_0 = 0$, see Fig. 1(e)) is not affected by edge scattering; (ii) the conductance of conductive non-zero conduction modes ($0 < |E_n| < |E_F| + kT$, see Fig. 1(e)) is strongly affected by edge scattering; (iii) non-zero conduction modes in neutral multi-layer zz-GNRs do not contribute to the total conductance because of their energy levels; (iv) several non-zero conduction modes in AsF_5 doped multi-layer zz-GNRs contribute significantly to the total conductance because of their energy levels, especially in case of specular edges. However, notable improvement occurs only when p is very close to 1 (e.g., $p > 0.8$ for $W = 16.5$ nm, **Fig. 11(b)**). This is because the zeroth conduction modes dominate the conductance for p not close to 1.

For local interconnects, where wire length can be comparable or smaller than l_D, the quantum contact resistance cannot be ignored. Similar to CNTs, the quantum contact resistance for GNRs is $h/2q^2$ for each conduction mode. The per unit length wire resistances as a function of length of different structures are shown in **Fig. 12**. It should be noted that the quantum contact resistance is the lower limit of contact resistance in CNT/GNR interconnects. In reality, the situation could be even worse, because of the imperfect contact resistance, which is fabrication technology dependent.

The delay of both global and local interconnects in 11 nm tech. node are analyzed based on the distributed *RLC* model in Fig. 5. For global interconnects (**Fig. 13**), the performance of mono-layer zz-GNR is much worse than Cu, while the multi-layer zz-GNR can match or become better than Cu only if it is intercalation (AsF_5) doped and have very specular edges ($p > 0.8$). The AsF_5 doped multi-layer zz-GNRs can even be better than SWCNT bundles if $p = 1$ is achieved. However, for more practical edge specularity, i.e., $p = 0.2$ to 0.6, GNRs cannot match the performance of Cu or that of SWCNT bundles (even for metallic fraction = 1/3) at the global level, till the very end of ITRS roadmap (11 nm tech. node). It is worth noting that for global interconnects, multi-walled CNT (MWCNT) bundles are better than SWCNT bundles (for metallic fraction = 1/3) [11], which implies that GNRs cannot match the performance of MWCNT bundles.

For local interconnects (**Fig. 14**), the performance of AsF_5 doped multi-layer zz-GNRs can match or even be better than that of Cu, depending on the specularity. The AsF_5 doped multi-layer zz-GNRs can be slightly better than SWCNT bundles if p=1 is achieved. Even the mono-layer zz-GNRs can be better than Cu in some special cases (minimum driver size and several micron wire lengths) due to their smaller capacitance. Also, the multi-layer zz-GNRs are better than tungsten in most cases, which suggest possible application of zz-GNRs for local interconnects. In general, till the very end of roadmap (11 nm tech. node), GNRs are not better than Cu, unless some special technology improvement is achieved (multi-layer zz-GNR with proper intercalation doping and very specular edges). The overall results are summarized in **Table 1**.

V. Summary

In this work, GNRs are analyzed from fundamental physics to their industrial prospects as VLSI interconnects. Mono-layer, neutral multi-layer and intercalation doped multi-layer zz-GNR interconnects are analyzed from both conductance and propagation delay perspectives. Although GNRs have some fabrication advantages over CNTs, they cannot match the performance of Cu or that of SWCNT bundles (with metallic fraction = 1/3) at the global level, from conductance and delay perspectives, till the very end of ITRS'07 roadmap (11 nm tech. node), unless some special technology improvements can be achieved (multi-layer zz-GNR with proper intercalation doping and very specular-edges). However, multi-layer zz-GNRs can be comparable to Cu at the local level (even for $p = 0$), and can have much better performance than that of tungsten, implying possible application as local interconnects.

Acknowledgment

This research is being supported by the National Science Foundation, Grant No. CCF-0811880.

References

[1] M. C. Lemme et al., *IEEE Elect. Dev. Lett.*, Vol. 28, No. 4, pp. 282-284, 2007.
[2] A. Naeemi et al., *IEEE Elect. Dev. Lett.*, Vol. 28, No. 5, pp. 428-431, 2007.
[3] A. Naeemi et al., *Proc IEEE Int. Interconnect Tech. Conf.*, 2008, pp. 183-185.
[4] L. X. Benedict et al., *Phys. Rev. B*, Vol. 52, No. 20, pp.14935-14940, 1995.
[5] A. K. Geim et al., *Nature Materials*, Vol. 6, pp. 183-191, 2007.
[6] D. A. Areshkin et al., *Nano Letters*, Vol. 7, No. 1, pp. 204-210, 2007.
[7] Intl. Tech. Roadmap for Semiconductors (ITRS), 2007, http://public.itrs.net
[8] S. Datta, *Electronic Transport in Mesoscopic Systems*, Cambridge Univ., 1995.
[9] C. Berger et al., *Science*, Vol. 312, No. 5777, pp. 1191-1196, 2006.
[10] J. Jiang et al., *Phys. Rev. B*, Vol. 64, No. 4, pp. 045409, 2001.
[11] H. Li et al., *IEEE Trans. Elect. Dev.*, Vol. 55, No. 6, pp. 1328-1337, 2008.
[12] J. E. Fischer et al., *Phys. Today*, Vol. 31, pp. 36-45, 1978.
[13] L. R. Hanlon et al., *Solid State Communications*, Vol. 24, pp. 377-381, 1977.
[14] M. S. Dresselhaus et al., *Advances in Phys.*, Vol. 51, No. 1, pp. 1-186, 2002.
[15] W. Steinhogl et al., *Microelectronic Engr.*, Vol. 82, pp. 266-272, 2005.
[16] M. Traving et al., *J. Appl. Phys.*, Vol. 100, No. 9, pp. 094325, 2006.
[17] J. Shioya et al., *Synthetic Metals*, Vol. 14, pp. 113-123, 1986.
[18] Predictive Technology Model (PTM), http://www.eas.asu.edu/~ptm/

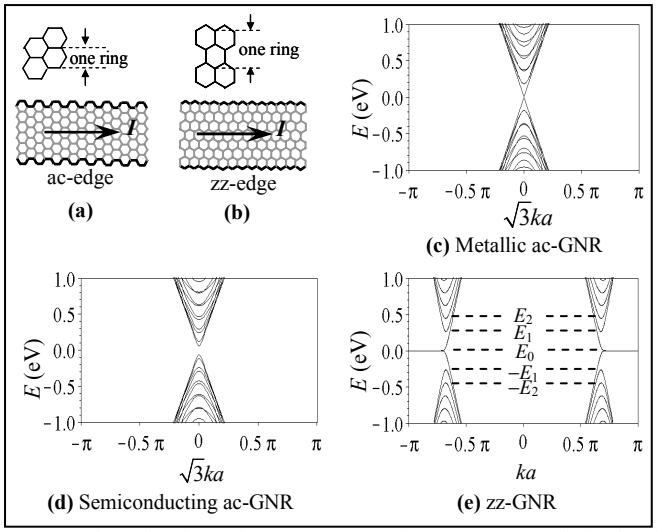

Fig. 1: Schematic view of **(a)** ac-GNR and **(b)** zz-GNR, and the band structures of **(c)** metallic ac-GNR (N = 44), **(d)** semiconducting ac-GNR (N=45) and **(e)** zz-GNR (N = 26) of similar width (11 nm). N is the number of hexagonal carbon rings across the width of GNR; a is the lattice constant (a = 0.246 nm). Note that kT is much less than ΔE_n (the difference in energy between any adjacent subbands).

$$G_n = \frac{2q^2}{h}\int T_n(E)\left(-\frac{\partial f_0}{\partial E}\right)dE \quad (1) \qquad f_0(E) = \left[1+\exp\left(\frac{E-E_F}{kT}\right)\right]^{-1}$$

$$T_n(E) = \left[1+L\left(\frac{1}{l_D\cos\theta}+\frac{1}{W\cot\theta}\right)\right]^{-1} \approx \frac{1}{L}\left(\frac{1}{l_D\cos\theta}+\frac{1}{W\cot\theta}\right)^{-1} \quad (2)$$

$$\cot\theta = v_{\parallel}/v_{\perp} = \sqrt{E^2-E_n^2}\,/\,|E_n|$$

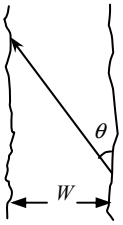

$$G_{total} = \sum_n G_n(electrons) + \sum_n G_n(holes) \quad (3)$$

$$G_{total} \approx \frac{2}{\Delta E_n}\left[\int_0^{\infty} G_n(electrons)dE_n + \int_{-\infty}^{0} G_n(holes)dE_n\right]$$

$$= \frac{1}{L}\frac{2q^2}{h}\cdot\frac{2W^2}{hv_f}\cdot 2kT\ln\left[2\cosh\left(\frac{E_F}{2kT}\right)\right]\cdot func(W,l_D) \quad (4)$$

$$func(W,l_D) = \begin{cases} \dfrac{\pi W-2l_D}{l_D} + \dfrac{4\sqrt{l_D^2-W^2}}{l_D}\cdot\operatorname{arctanh}\left(\sqrt{\dfrac{l_D-W}{l_D+W}}\right), & l_D \ge W \\ \dfrac{\pi W-2l_D}{l_D} - \dfrac{4\sqrt{W^2-l_D^2}}{l_D}\cdot\arctan\left(\sqrt{\dfrac{W-l_D}{W+l_D}}\right), & l_D < W \end{cases}$$

$$\approx \begin{cases} 2\ln(l_D/W) + 2\ln 2 - 2 + \pi W/l_D, & l_D >> W \\ \pi l_D/2W - 2l_D^2/3W^2, & l_D << W \end{cases}$$

$$G_{sheet} = \lim_{W\to\infty}\frac{LG_{total}}{W} = \frac{2q^2}{h}\cdot\frac{\pi l_D}{hv_f}\cdot 2kT\ln\left[2\cosh\left(\frac{E_F}{2kT}\right)\right] \quad (5)$$

Fig. 2: Derivation of the general expression for a single GNR layer's conductance (assuming complete diffusive-edge). G_n is the conductance of the n^{th} conduction mode (with consideration of spin); $T_n(E)$ is the transmission coefficient (the approximation is valid when $L>>l_D$); $f_0(E)$ is Fermi-Dirac distribution function; E_F is the the Fermi Level; L and W are the length and width of the GNR, respectively; l_D is the MFP corresponding to scatterings by defects and phonons (not edge scattering); $\cot\theta$ is the ratio of longitudinal and transverse velocities (shown in the inset); E_n is the minimum (maximum) energy of the n^{th} conduction (valence) subband (for zz-GNRs, E_0 = 0 and $|E_n|$ = ($|n|$ + 1/2) $hv_f/2W$ for $n\neq 0$ [3], where h is Planck's constant, and $v_f = 10^6$ m/s is the Fermi velocity); G_{total} is the total conductance; G_{sheet} is the 2D sheet conductance of graphene.

$l_D(\text{armchair CNT}) = \pi D\cdot\sqrt{3}\gamma^2/\left(2\sigma_\varepsilon^2+9\sigma_\gamma^2\right)$ [10]

$\gamma = -2.7\text{eV}$ $\qquad l_D(\text{CNT}) \approx 1000D$ [11]

$l_D(\text{metallic ac-GNR}) = 2(N+1)d_0\left(\gamma^2-E^2/4\right)/\left(\sigma_\varepsilon^2+4\sigma_\gamma^2\right)$ (based on [6])

$\approx \left(2W/\sqrt{3}\right)\left(\gamma^2-E^2/4\right)/\left(\sigma_\varepsilon^2+4\sigma_\gamma^2\right) \approx (4W/3)\cdot\sqrt{3}\gamma^2/\left(2\sigma_\varepsilon^2+8\sigma_\gamma^2\right)$

l_D(zz-GNR) is comparable to l_D(metallic ac-GNR) for similar W [6];

l_D(GNR) can be approximated as l_D(GNR)≈450W, analogous to CNTs.

Fig. 3: l_D modeling of GNRs based on the analogy between CNTs and GNRs; σ_ε and σ_γ are the variances; d_0 = 0.142 nm is the C-C bond length; D is the diameter of CNT; E is the energy (E << γ); N is defined in Fig. 1, which is different from the one defined in [6], leading to a prefactor of 2.

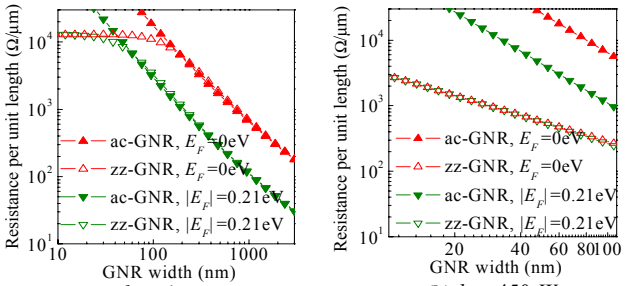

Fig. 4: Resistance of both neutral (E_F = 0 eV) and charged ($|E_F|$ = 0.21 eV [2]) mono-layer ac- and zz-GNRs, assuming **(a)** l_D = 1 μm and **(b)** l_D = 450 W.

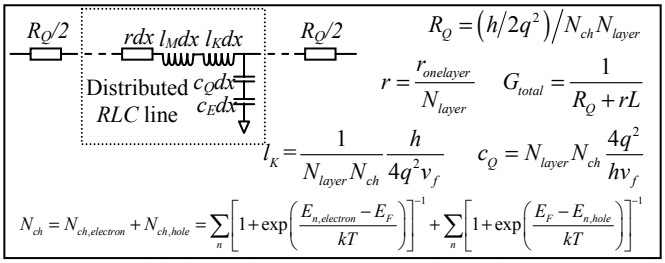

$$R_Q = \left(h/2q^2\right)/N_{ch}N_{layer} \qquad r = \frac{r_{onelayer}}{N_{layer}} \qquad G_{total} = \frac{1}{R_Q+rL}$$

$$l_K = \frac{1}{N_{layer}N_{ch}}\frac{h}{4q^2v_f} \qquad c_Q = N_{layer}N_{ch}\frac{4q^2}{hv_f}$$

$$N_{ch} = N_{ch,electron} + N_{ch,hole} = \sum_n\left[1+\exp\left(\frac{E_{n,electron}-E_F}{kT}\right)\right]^{-1} + \sum_n\left[1+\exp\left(\frac{E_F-E_{n,hole}}{kT}\right)\right]^{-1}$$

Fig. 5: *RLC* model of GNR interconnects (assuming perfect contact). N_{ch} is the number of conducting channels (modes) in one layer; R_Q is the quantum contact resistance; r is the distributed scattering resistance; c_Q and c_E are the quantum and electrostatic capacitance, respectively; l_K and l_M are the kinetic and magnetic inductance, respectively; N_{layers} is the number of GNR layers.

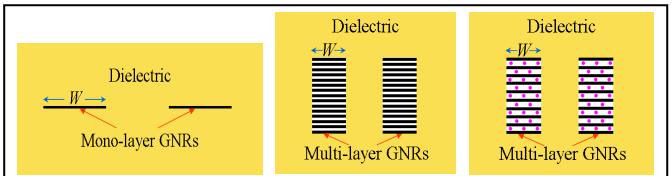

Fig. 6: Schematic view of **(a)** mono-layer GNRs, and **(b)** neutral and **(c)** intercalation doped multi-layer GNRs (graphite).

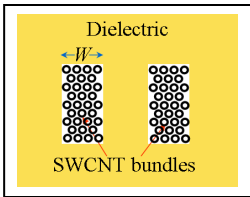

$$G(\text{Single metallic SWCNT}) \approx \frac{1}{L}\frac{4q^2l_D}{h}$$

$$\sigma(\text{SWCNT bundles}) \approx \frac{1}{3}\frac{4q^2l_D/h}{(D+s)^2\sqrt{3}/2}$$

when s = 0.34 nm and D = 1 nm, l_D = 1 μm and σ(SWCNT bundles) = 0.33 (μΩ cm)$^{-1}$.

Fig. 7: Schematic view and the conductivity model of SWCNT bundles. The prefactor 1/3 arises from the approximation that 1/3 of the CNTs are metallic. D is the diameter of a single SWCNT; s is the minimum spacing between adjacent SWCNTs; σ is the conductivity.

$$\rho = \rho_0 \left\{ \frac{1}{3} \Big/ \left[\frac{1}{3} - \frac{\alpha}{2} + \alpha^2 - \alpha^3 \ln\left(1 + \frac{1}{\alpha}\right) \right] + \frac{3}{8} C(1-p) \frac{1 + AR}{AR} \frac{l_D}{W} \right\}$$

$$\alpha = (l_D / d) R/(1-R) \quad d = W/2 \quad C = 1.2 \quad R = 0.25 \quad p = 0.3$$

$$\rho_0 = 8.7\ \mu\Omega\text{cm} \quad l_D = 33\ \text{nm}$$

Fig. 8: Resistivity model for tungsten. ρ_0 is the resistivity of the bulk material; AR is the aspect ratio; W is the width; l_D is the mean free path; d is the average distance between grain boundaries; p is the specularity parameter, and R is the reflectivity coefficient at grain boundaries [15, 16].

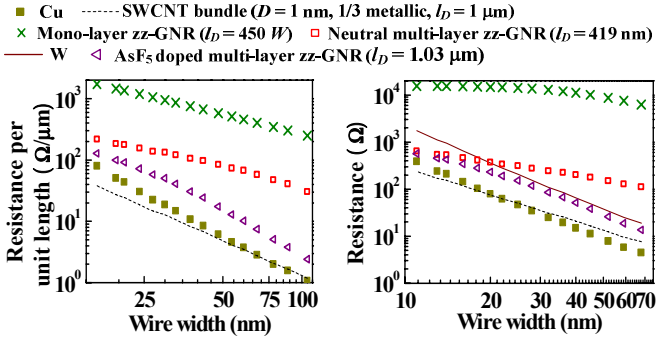

(a) Long global wires **(b)** Local wires (L = 1 μm)

Fig. 9: Resistance comparison of **(a)** global and **(b)** local wires among Cu, W, SWCNT bundles and different types of GNRs. For mono-layer GNRs, l_D = 450 W and $|E_F|$ = 0.21 eV; for neutral multi-layer GNRs, l_D = 419 nm (fixed); for stage 2 AsF_5 doped multi-layer GNRs, average layer spacing is 0.575 nm, fixed l_D = 1.03 μm and $|E_F|$ = 0.60 eV. Specularity (p) is assumed to be zero.

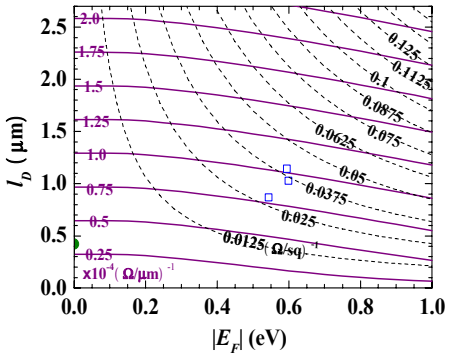

Fig. 10: Conductance contours as a function of Fermi Level, $|E_F|$ and MFP, l_D. Solid lines show the conductance per layer of 16.5 nm wide (minimum global wire width in 11 nm tech. node) multi-layer zz-GNRs. Dashed lines show the sheet conductance per layer of graphite. The "dot" on the lower left hand side represents neutral graphite, while the "open squares" represent the three stages of AsF_5 intercalation doped graphite [13].

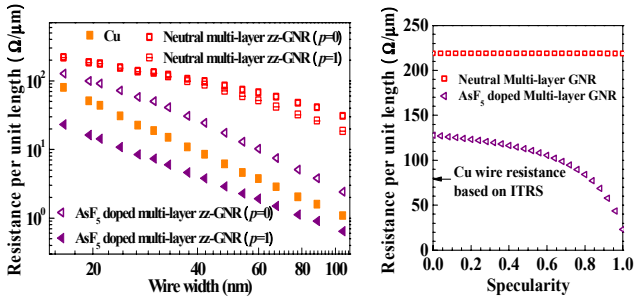

(a) Resistance vs. width **(b)** Resistance vs. specularity

Fig. 11: Impact of edge specularity of multi-layer zz-GNRs on long global wire's resistance: **(a)** resistance vs. width and **(b)** resistance vs. specularity (W = 16.5 nm, AR = 2.9).

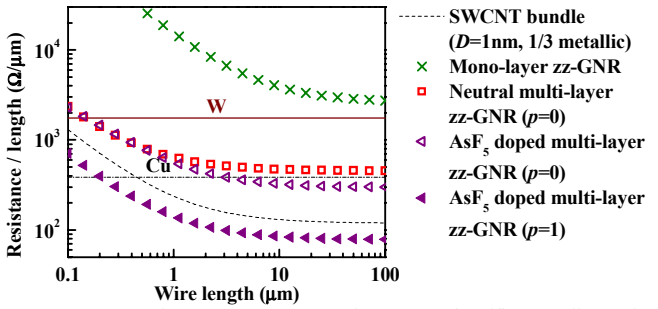

Fig. 12: Impact of quantum contact resistance on local/intermediate wire resistance (W = 11 nm, AR = 2.1).

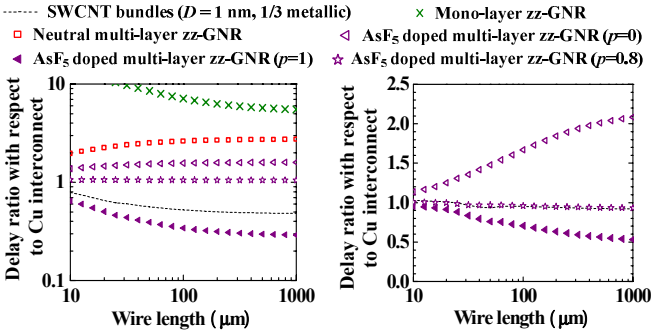

(a) Minimum wire width (16.5 nm) **(b)** Wire width of 82.5 nm

Fig. 13: *RLC* delay ratio (at 11 nm tech. node) with respect to Cu wire for global interconnects (H = 2.9x16.5 nm); 50 times minimum sized driver and load), with wire width of: **(a)** minimum value = 16.5 nm, and **(b)** 82.5 nm (curves for mono-layer and neutral multi-layer zz-GNRs are out of range). The kinetic inductances and quantum capacitances are obtained by using the model shown in **Fig. 5**, while magnetic inductances and electrostatic capacitances are obtained from PTM model [18]. Simulations were implemented using HSPICE.

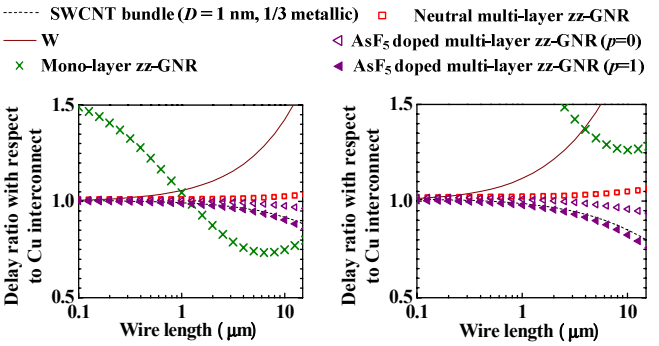

(a) Minimum driver size **(b)** Double of minimum driver size

Fig. 14: *RLC* fanout-of-4 delay ratio with respect to Cu wire for local interconnects (W = 11 nm, AR = 2.1), with **(a)** minimum driver size and **(b)** twice the minimum driver size. (The driver equivalent resistance and capacitance are obtained from the 11 nm tech. node, ITRS 2007 [7]).

Table 1 Performance comparison of different materials with respect to Cu at 11 nm tech. node of ITRS'07.

Interconnect material	Global	Local
W	-	Worse
SWCNT (D=1nm, 1/3 metallic)	Better	Better
Mono-layer GNR	Much worse	Worse for most cases
Neutral multi-layer GNR	Worse	Slightly worse
AsF_5 doped multi-layer GNR (p=0)	Worse	Comparable
AsF_5 doped multi-layer GNR (p=1)	Much better	Better